Dispersion-Induced Dynamical Transition in Parametric Solitary Waves

Antonio Picozzi[1] and Marc Haelterman[2]

[1]CNRS, Laboratoire de Physique de la Matière Condensée, Université de Nice Sophia-Antipolis, 06108 Nice, France

[2]Service d'Optique et d'Acoustique, Université Libre de Bruxelles, 50 Avenue F.D. Roosevelt, C.P. 194/5, B-1050 Brussels, Belgium

(Received 7 May 1999)

We investigate the influence of dispersion on parametric solitary waves. We show that dispersion is responsible for a transition towards a new type of dynamical solitary wave characterized by the presence of traveling phase defect arrays within their envelopes. The transition is described analytically through an original extension of the Kolmogorov-Petrovskii-Piskunov approach to front propagation into unstable states.

PACS numbers: 42.65.Tg, 05.45.Yv, 42.65.Ky, 42.65.Re

Parametric wave mixing processes play an important role in many physical systems. They generally take place in weakly nonlinear media characterized by either quadratic or cubic nonlinearities and are thus encountered in such diverse fields as plasma physics, fluid dynamics, and nonlinear optics. The development of analytical tools for solving the governing equations of these processes has led to the discovery of parametric solitary waves [1–5]. These solitary waves consist of steady-state field envelopes resulting from a balance between the energy exchanges due to the parametric interaction and the group velocity difference between the interacting waves.

Apart from the group velocity difference, dispersion effects on the interacting waves has been systematically ignored in previous theoretical studies of parametric solitary waves. We show in the present Letter that this systematic omission is not valid and that even very weak dispersion can drastically alter the parametric solitary waves dynamics. In particular, we show that dispersion induces a dynamical transition of the parametric solitary waves that results in the formation of moving periodic patterns across their field envelopes.

The periodic patterns consist of arrays of phase defects whose amplitude profiles result from a balance between dispersion and nonlinearity in a way similar to what happens in symbiotic quadratic solitary waves encountered in nonlinear optics [6,7]. The symbiotic solitary waves consist of another type of nonlinear waves sustained by a parametric interaction. They result from a balance between dispersion and nonlinearity in the absence of net energy exchange between the interacting waves and thus do not require walk-off, unlike parametric solitary waves. However, symbiotic solitary waves were shown to persist in the presence of walk-off leading to the so-called walking solitons [8]. Both bright [6] and dark [7] optical symbiotic solitary waves have been predicted theoretically. The new class of solitary wave that results from the dynamical transition can therefore be viewed as exhibiting a hybrid parametric and symbiotic nature: the envelope resulting from net parametric energy exchanges and walk-off is modulated by a walking periodic array of symbiotic dark solitons resulting from a balance between dispersion and nonlinearity.

We present the new dynamical solitary wave in the context of nonlinear optics. The dynamical transition is described analytically from an original extension of the Kolmogorov-Petrovskii-Piskunov (KPP) conjecture [9]. The main idea behind our approach is to treat the solitary wave dynamics as a problem of front propagation into unstable states as described by the so-called marginal stability theory recently developed in various contexts [10,11].

For concreteness, we study the degenerate phase-matched three-wave parametric interaction that couples a fundamental wave and its second harmonic in a quadratic nonlinear optical crystal. The slowly varying amplitude envelopes u_1 and u_2 of the signal and pump waves of frequencies ω_1 and $\omega_2 = 2\omega_1$, respectively, are ruled by the following dimensionless equations

$$\frac{\partial u_1}{\partial t} - \frac{\partial u_1}{\partial x} + \mu_1 u_1 = u_2 u_1^* - i\beta_1 \frac{\partial^2 u_1}{\partial x^2}, \tag{1a}$$

$$\frac{\partial u_2}{\partial t} + \frac{\partial u_2}{\partial x} + \mu_2 u_2 = -\rho u_1^2 - i\beta_2 \frac{\partial^2 u_2}{\partial x^2}, \tag{1b}$$

where x and t are, respectively, the longitudinal space coordinate and the time in a reference frame traveling at the average velocity $(v_1 + v_2)/2$, where v_i are the velocities of the signal and pump waves. We consider a configuration in which the amplitude of the pump wave is kept constant at the crystal input face and we normalize the problem with respect to this amplitude, for instance, e_0 in real units. The variables can be recovered in real units through the transformations $u_i \to u_i e_0$, $t \to t/(\sigma_1 e_0)$, $\alpha_i \to \mu_i(\sigma_1 e_0)$, and $x \to x\delta/(\sigma_1 e_0)$, where $\delta = (v_2 - v_1)/2$, α_i are the damping rates representing the effects of crystal absorption at both frequencies, and σ_i is the parametric coupling constant $\sigma_i = d|v_i|\omega_i/(cn_i)$, n_i and d being the refractive index $n_i = n(\omega_i)$ and the effective nonlinear susceptibility, respectively. The nonlinear coefficient in Eq. (1b) is the ratio $\rho = \sigma_2/\sigma_1$. The effects of dispersion are represented by the second derivatives with respect to the spatial variable x so that the dispersion parameters are given in terms of real unit parameters by $\beta_i = |v_i|^3 k_i'' \sigma_1 e_0 / 2\delta^2$, where $k_i'' = (\partial^2 k/\partial\omega^2)_i$, k

 0031-9007/00/84(25)/5760(4)$15.00

being the wave vector modulus, $k = n(\omega)\omega/c$. For simplicity, we assume in the following that $\beta = \beta_2 = \beta_1$, $\rho = 2$ and $v_1 < v_2$. These assumptions do not affect the generality of our results.

In the absence of dispersion ($\beta = 0$), the three-wave interaction model has been extensively studied in the literature. In particular, for the conservative case $\mu_1 = \mu_2 = 0$, analytical solitary-wave solutions have been derived in the form of a sech-shaped envelope for the signal wave and a tanh-shaped envelope for the pump wave [1]. This solution has been generalized to the dissipative case under the assumption that the pump loss μ_2 is negligible with respect to the signal loss μ_1 so that one can set $\mu_2 = 0$ in Eq. (1) [2,3]. We consider here this situation for which a solitary-wave solution always exists provided that $\mu_1 < 1$.

Our scope is to study the influence of dispersion on the parametric solitary wave. To this end, we numerically solve Eq. (1) with $\beta \neq 0$ and with an initial sech-shaped envelope for the signal. Our results are illustrated in Fig. 1 for the initial condition $u_1(x, t = 0) = 0.1\,\mathrm{sech}(q_0 x)$ with $q_0 = 70$, $u_2(x, t = 0) = 1$, and a damping $\mu_1 = 0.6$. The amplitude envelopes are shown in the reference frame traveling at the signal group velocity defined by $z = x + t, \tau = t$. The case of Figs. 1(a) and 1(b) corresponds to a small value of the dispersion parameter, $\beta = 2 \times 10^{-5}$. After some transients, the interacting fields self-structurate, giving rise to the usual parametric solitary wave (Fig. 1b) where the signal loss μ_1 is compensated by the incoming pump. The expected envelope reshaping induced by the dispersion is almost invisible. One would be tempted to explain this merely by the fact that a small value of β corresponds to a situation where walk-off effects predominate over dispersion. However, the numerical example of Figs. 1(c) and 1(d) reveals quite remarkably that this usual criterion for neglecting dispersion does not hold. Indeed, Figs. 1(c) and 1(d) show the case of a slightly larger dispersion parameter, $\beta = 2.5 \times 10^{-5}$, with the same initial conditions as in Fig. 1(a). We see that dispersion is responsible for a transition characterized by the appearance of a dynamical periodic pattern in the solitary-wave envelope. A detailed analysis shows that the pattern is generated from the drift of π-phase defects that appear periodically in the leading front of the signal pulse. This is illustrated in Fig. 2 which shows the phase profile of the signal wave. The drift of the phase defects can be easily explained physically from the fact that they constitute symbiotic solitary waves of the dark type that propagate approximately at the group velocity of the signal wave that is weaker than the velocity of the solitary wave that is superluminous [2]. Note that the phase defects have not been observed in previous studies of dispersion effects in parametric solitary waves [2d,4] because the nondegenerate configuration considered in those works prevents them from appearing due to the inherent group velocity difference between the signal and idler fields.

This mechanism of pattern formation through phase alternation is similar to that occurring in bistable systems described by a generalized Fisher-Kolmogorov equation [11] as well as in the optical parametric oscillator [12]. In those systems, however, the fronts propagate between two homogeneous states, while here the signal amplitude undergoes a continuous evolution induced by the energy transfer with the pump, which is the reason why the overall shape of the resulting dynamical solitary wave is reminiscent of the dispersionless solitary wave.

This brief discussion on the origin of the pattern forming transition in dispersive parametric solitary waves suggests the application of the KPP approach. The KPP approach has already been successfully applied to the characterization of optical solitary waves associated with stimulated Brillouin scattering [3] and three-wave parametric interactions [4]. We generalize here the approach to include the description of the dispersion-induced dynamical transition. The method consists in describing the properties of a front propagating into an unstable state from a linear analysis of

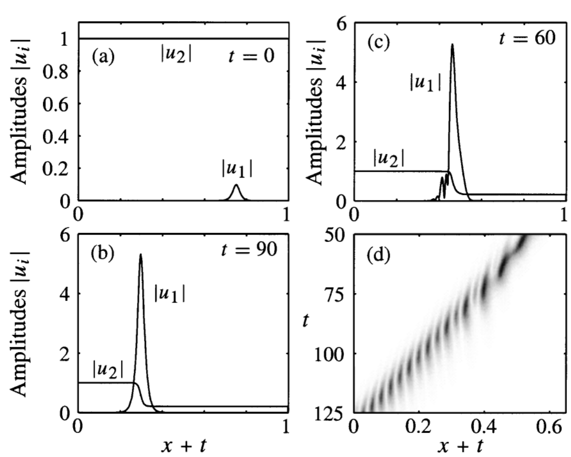

FIG. 1. Evolution of the envelopes $u_{1,2}$ in the reference frame of the signal wave (amplitudes are given in units of e_0, $\mu_2 = 0$). (a,b) Parametric solitary wave generation from $t = 0$ to $t = 90$; (c) dynamical solitary wave generation, transient at $t = 60$; (d) density plot showing the overall evolution.

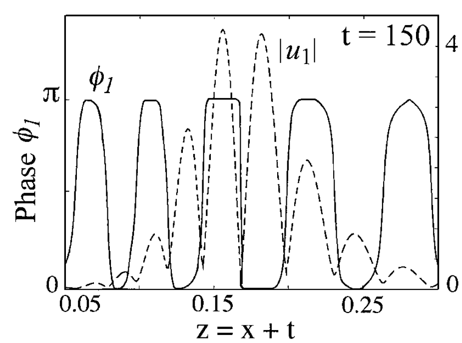

FIG. 2. Phase (solid line) and amplitude (dashed line) of the signal component of the dynamical solitary wave for the parameters of Fig. 1 ($u_1 = |u_1|e^{i\phi_1}$).

the leading edge of the front profile. We therefore start our analysis from the undepleted pump regime for which we can linearize Eq. (1) around the trivial unstable solution $u_1(x,t) = 0, u_2(x,t) = 1$. Assuming a signal wave of the form $u_1(x,t) = \tilde{u}_1 \exp(\gamma t + iqx)$, the linearized Eq. (1) provides the following dispersion relation

$$\gamma(q) = iq - \mu_1 + \sqrt{1 - \beta^2 q^4}, \tag{2}$$

where we keep only the positive sign of the square root corresponding to a potentially unstable root $\mathrm{Re}(\gamma) > 0$. The general solution to the linearized Eq. (1) in a reference frame ($\xi = x + Vt, \tau = t$) traveling at the velocity of the solitary wave V has the form

$$u_1(\xi,\tau) = \int_{-\infty}^{+\infty} \tilde{u}_1(q) \exp\{[\gamma(q) - iqV]\tau\} \exp(iq\xi)\, dq, \tag{3}$$

where $\tilde{u}_1(q)$ is the Fourier transform of the initial signal field $u_1(\xi, \tau = 0)$. In the spirit of the KPP approach, this field can be reduced to the exponential leading front of the sech-shaped solitary wave under study, $u_1(\xi, \tau = 0) \propto \exp(q_0 \xi)$. The function $\tilde{u}_1(q)$ then possesses a pole on the imaginary axis in $q = -iq_0$. On the other hand, the function $f(q) = \gamma(q) - iqV$ has a saddle point q_s defined through the relation

$$\left.\frac{\partial \gamma(q)}{\partial q}\right|_{q_s} = iV. \tag{4}$$

The KPP procedure presented below reveals that this saddle point is responsible for a velocity selection of the solitary wave. Therefore, for the sake of simplicity and without loss of rigor, we can from now consider the saddle point q_s at this particular selected velocity $V = V^*$ given in Eq. (9). One finds, in a first order approximation in terms of βq^2, $q_s = \omega - i\sigma$, where $\sigma = (1 - \mu_1)^{1/4}/(12^{1/4}|\beta|^{1/2})$ and $\omega = \sqrt{3}\sigma$.

To calculate the integral Eq. (3), we continue the integrand over the complex q plane and apply the Cauchy theorem according to which the integration can be performed along any contour C different from the real axis, provided that the integrand is analytic in the domain D bounded by this new contour and the real axis. In particular, we can calculate the integral on a contour C that goes through the saddle point q_s, as depicted in Fig. 3, so that the result can be provided by the steepest descent method. Note that, due to the presence of the square root in γ, the integrand exhibits four branch cuts that can always be chosen so that they do not cross the contour C since the lower branch point $q = -i/\sqrt{|\beta|}$ is always below the saddle point q_s, i.e., $1/\sqrt{|\beta|} > \sigma$. However, when the dispersion $|\beta|$ is so small that $\sigma > q_0$, the contour has to go around the pole and both the saddle point and the pole contribute to the integral that can thus be written as

$$u_1(\xi,\tau) \propto I_{\mathrm{pol}} + I_{\mathrm{sad}}, \tag{5}$$

where I_{pol} is given by the residue

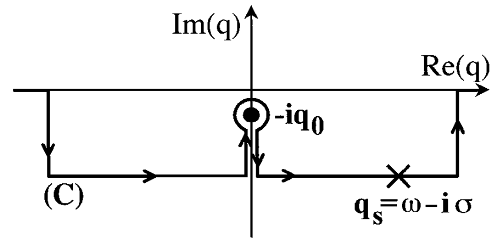

FIG. 3. Contour C in the complex q plane.

$$I_{\mathrm{pol}} \propto \exp[f(q = -iq_0)\tau] \exp(q_0\xi), \tag{6}$$

while I_{sad} is calculated by the steepest descent method that yields

$$I_{\mathrm{sad}} \propto \tilde{u}_1(q_s) \exp[f(q_s)\tau] \exp[(\sigma + i\omega)\xi]. \tag{7}$$

The long term behavior of the solution will then be dominated by the pole or the saddle depending on the values of $\mathrm{Re}[f(q)]$ in $q = -iq_0$ and q_s. The pole dominates when $\mathrm{Re}[f(q = -iq_0)] > \mathrm{Re}[f(q = q_s)]$, namely, when

$$|\beta| < \beta_t = \frac{3^{3/2}}{2^5} \frac{\sqrt{1 - \mu_1}}{q_0^2}. \tag{8}$$

For the numerical example of Fig. 1, one finds $\beta_t = 2.1 \times 10^{-5}$. If β is smaller than the threshold value β_t, the pole dominates and one finds the standard result of the KPP approach to front propagation problems according to which the system exhibits a one-parameter family of dispersive parametric solitary waves whose velocities are determined by the initial leading front slope q_0 [1–3]. These are the solutions illustrated in Figs. 1(a) and 1(b).

The problem of interest here is to investigate what happens when the dispersion increases above the threshold value β_t as in Figs. 1(c) and 1(d). In that case, the saddle point contribution becomes dominant and Eq. (7) indicates that there exists a velocity V for which the solution neither grows nor decays; i.e., $\mathrm{Re}[f(q = q_s)] = 0$. This stationarity condition fixes the solitary wave velocity to a particular value V^* independent of the initial condition,

$$V^* = 1 + \frac{2^{5/2}}{3^{3/4}} |\beta|^{1/2} (1 - \mu_1)^{3/4}. \tag{9}$$

Because the dominating saddle point is a complex number $q_s = \omega - i\sigma$, Eq. (7) describes an exponential front of slope σ accompanied by a periodic modulation responsible for the generation of a periodic array of phase defects in the signal envelope. By assuming the conservation of the flux of phase defects when passing from the linear to the nonlinear stage of their evolution within the envelope [11], we can derive the period of the array $\lambda = \pi(V^* - 1)/[\mathrm{Im}(\gamma^*) - \omega V^*] = \pi 2^{5/2} \beta^{1/2}/[3^{5/4}(1 - \mu_1)^{1/4}]$.

All the theoretical predictions that characterize the dynamical transition, i.e., the dispersion threshold β_t, the selected velocity V^*, the front slope σ, and the array period λ, were found to be in excellent agreement with the numerical simulations. Note that the nature of the present dynamical transition is fundamentally different from that reported in Ref. [11]. Indeed, in that previous work the dynamical transition is due to the emergence of the saddle point, while it results here from a competition between a pole and a permanent saddle point.

When dispersion becomes so large that $\sigma < q_0$, i.e., when $|\beta| > 16\beta_t/9$, the pole no longer contributes to the integral and the solitary wave keeps unconditionally its dynamical nature. Similarly, if the initial condition does not include an exponential front for the signal wave, the pole q_0 no longer exists and the saddle point is isolated in the above analysis. Consequently, no competition can occur and the dynamical solitary waves are unconditionally formed. Accordingly, we have verified numerically the generation of dynamical parametric solitary waves, at arbitrarily small values of β, for Gaussian signal envelopes as initial conditions. Our results reveal that the dynamical solitary wave constitutes a robust attractor of the system, which should facilitate its experimental observation. Note that, quite remarkably, since the period of the phase defect array λ is proportional to $\beta^{1/2}$, the influence of dispersion on parametric solitary waves appears to be more effective for lower dispersion values.

For larger values of β, we have observed a second transition induced by a modulational instability whose study is beyond the scope of the present Letter. Modulational instability is indeed unavoidable when dispersion dominates over walk-off effects [5]. In order to avoid the onset of modulational instability in practice, we suggest a quasi-phase-matched backward configuration [13] for the experimental observation of the dynamical parametric solitary waves. In the backward configuration we have $v_2 > 0$ and $v_1 < 0$ so that walk-off effects are large enough to dominate the natural dispersion of optical quadratic materials. In this situation, the simulation reported in Figs. 1(c) and 1(d) corresponds to a 230 fs sech-shaped signal pulse propagating in a 6 cm long quasi-phase-matched crystal with an effective nonlinearity $d = 35$ pm/V, a loss coefficient $\alpha_1 = 9.4\ \mathrm{cm}^{-1}$ and a typical dispersion $k'' = 1.7\ \mathrm{ps}^2/\mathrm{m}$. The corresponding intensity of the counter-propagating continuous pump is $I = 200\ \mathrm{MW/cm}^2$. The simulation of Figs. 1(c) and 1(d) reveals that, thanks to the backward configuration, the dynamical solitary wave can, in principle, be generated in a single pass configuration.

In summary, by means of an original extension of the KPP approach to front propagation into unstable states, we described analytically the dynamical transition that affects parametric solitary waves owing to the effects of dispersion on their constituent interacting waves. The transition results from a competition between the pole associated with the exponential front of the solitary wave and the saddle point introduced by dispersion into the linearized problem. The transition occurs between a one-parameter family of parametric solitary waves and a velocity selected hybrid solitary wave whose envelope is characterized by a walking periodic array of phase defects analogous to dark topological solitons. Although the theory has been developed in the context of nonlinear optics for the particular case of a degenerate three-wave interaction, the great generality of our mathematical treatment suggests that the phenomenon described here is ubiquitous in physics. We can reasonably expect, in the near future, the experimental observation of the dynamical solitary wave in the context of nonlinear optics, thanks to the recent progress made on quasi-phase-matched quadratic materials.

A. P. thanks J. L. Meunier, C. Montes, and S. Coen for their valuable comments and help in this work.

[1] D. J. Kaup, A. Reiman, and A. Bers, Rev. Mod. Phys. **51**, 275 (1979); J. A. Armstrong, S. S. Jha, and N. S. Shiren, IEEE J. Quantum Electron. **6**, 123 (1970); S. C. Chiu, J. Math. Phys. **19**, 168 (1978); K. Nozaki and T. Taniuti, J. Phys. Soc. Jpn. **34**, 796 (1973); K. Druhl, R. G. Wenzel, and J. L. Carlsten, Phys. Rev. Lett. **51**, 1171 (1983).

[2] (a) E. Picholle *et al.*, Phys. Rev. Lett. **66**, 1454 (1991); (b) S. F. Morozov *et al.*, Sov. J. Quantum Elctron. **8**, 576 (1978); (c) A. D. D. Craik *et al.*, Wave Motion **15**, 173 (1992); (d) A. Picozzi and M. Haelterman, Opt. Lett. **23**, 1808 (1998).

[3] C. Montes *et al.*, Phys. Rev. E **55**, 1086 (1997); C. Montes, A. Picozzi, and D. Bahloul, Phys. Rev. E **55**, 1092 (1997).

[4] A. Picozzi and M. Haelterman, Europhys. Lett. **45**, 463 (1999).

[5] S. Trillo, Opt. Lett. **21**, 1111 (1996).

[6] See, e.g., Yu. N. Karamzin and A. P. Sukhorukov, JETP Lett. **20**, 339 (1974); M. J. Werner and P. D. Drummond, J. Opt. Soc. Am. B **10**, 2390 (1993); Y. Chen and J. Atai, Opt. Lett. **19**, 1287 (1994); D. E. Pelinovsky, A. V. Buryak, and Y. S. Kivshar, Phys. Rev. Lett. **75**, 591 (1995); A. V. Buryak, Y. S. Kivshar, and S. Trillo, Phys. Rev. Lett. **77**, 5210 (1996); P. Di Trapani *et al.*, Phys. Rev. Lett. **81**, 570 (1998).

[7] K. Hayata and M. Koshiba, Phys. Rev. A **50**, 675 (1994); A. V. Buryak and Y. S. Kivshar, Phys. Rev. A **51**, R41 (1995); S. Trillo and P. Ferro, Opt. Lett. **20**, 438 (1995).

[8] L. Torner *et al.*, Phys. Rev. Lett. **77**, 2455 (1996); D. Mihalache *et al.*, Phys. Rev. E **56**, R6294 (1997).

[9] V. G. Kolmogorov, I. G. Petrovskii, and N. S. Piskunov, Bull. Univ. Moscow, Ser. Int. Sec. A **1**, 1 (1937).

[10] J. S. Langer, Rev. Mod. Phys. **52**, 1 (1980).

[11] G. Dee and J. S. Langer, Phys. Rev. Lett. **50**, 383 (1983); G. Dee and W. van Saarloos, Phys. Rev. Lett. **60**, 2641 (1988).

[12] M. Santagiustina *et al.*, Opt. Lett. **23**, 1167 (1998); M. Taki, M. San Miguel, and M. Santagiustina, Phys. Rev. E **61**, 2133 (2000).

[13] J. U. Kang *et al.*, Opt. Lett. **22**, 862 (1997); G. D'Alessandro, P. St. J. Russell, and A. A. Wheeler, Phys. Rev. A **55**, 3211 (1997).